

## **Integrated Modeling and Analysis of Physical Oceanographic and Acoustic Processes**

Timothy F. Duda  
Applied Ocean Physics and Engineering Department, MS 11  
Woods Hole Oceanographic Institution  
Woods Hole, MA 02543  
phone: (508) 289-2495 fax: (508) 457-2194 email: [tduda@whoi.edu](mailto:tduda@whoi.edu)

James F. Lynch  
Applied Ocean Physics and Engineering Department, MS 11  
Woods Hole Oceanographic Institution  
Woods Hole, MA 02543  
phone: (508) 289-2230 fax: (508) 457-2194 email: [jlynch@whoi.edu](mailto:jlynch@whoi.edu)

Ying-Tsong Lin  
Applied Ocean Physics and Engineering Department, MS 11  
Woods Hole Oceanographic Institution  
Woods Hole, MA 02543  
phone: (508) 289-2329 fax: (508) 457-2194 email: [ytlin@whoi.edu](mailto:ytlin@whoi.edu)

Karl R. Helfrich  
Physical Oceanography Department, MS 21  
Woods Hole Oceanographic Institution  
Woods Hole, MA 02543  
phone: (508) 289-2870 fax: (508) 457-2181 email: [khelfrich@whoi.edu](mailto:khelfrich@whoi.edu)

Weifeng Gordon Zhang  
Applied Ocean Physics and Engineering Department, MS 11  
Woods Hole Oceanographic Institution  
Woods Hole, MA 02543  
phone: (508) 289-2521 fax: (508) 457-2194 email: [wzhang@whoi.edu](mailto:wzhang@whoi.edu)

Harry L. Swinney  
Department of Physics, C1610  
University of Texas at Austin  
Austin TX 78712  
phone: (512) 471-4619 fax: (512) 471-1558 email: [swinney@chaos.utexas.edu](mailto:swinney@chaos.utexas.edu)

John Wilkin  
Department of Marine and Coastal Sciences,  
Rutgers University  
New Brunswick, NJ 08901-8521  
phone: (848) 932-3366 fax: (732) 932-8578 email: [jwilkin@rutgers.edu](mailto:jwilkin@rutgers.edu)

Pierre F. J. Lermusiaux  
Department of Mechanical Engineering  
Massachusetts Institute of Technology  
Cambridge, MA 02139  
phone: (617) 324-5172 fax: (617) 324-3451 email: [pierrel@mit.edu](mailto:pierrel@mit.edu)

Nicholas C. Makris  
Massachusetts Institute of Technology  
77 Massachusetts Avenue, Room 5-222  
Cambridge, MA 02139  
phone: (617) 258-6104 fax: (617) 253-2350 email: [makris@mit.edu](mailto:makris@mit.edu)

Dick K. P. Yue  
Department of Mechanical Engineering  
Massachusetts Institute of Technology  
Cambridge, MA 02139  
phone: (617) 253- 6823 fax: (617) 258-9389 email: [yue@mit.edu](mailto:yue@mit.edu)

Mohsen Badiy  
College of Earth, Ocean, and Environment  
University of Delaware  
Newark, DE 19716  
phone: (302) 831-3687 fax: (302) 831-3302 email: [badiy@udel.edu](mailto:badiy@udel.edu)

William L. Siegmann  
Department of Mathematical Sciences  
Rensselaer Polytechnic Institute  
Troy, New York 12180-3590  
phone: (518) 276-6905 fax: (518) 276-2825 email: [siegmw@rpi.edu](mailto:siegmw@rpi.edu)

Jon M. Collis  
Applied Mathematics & Statistics  
Colorado School of Mines  
Golden, CO 80401  
phone: (303) 384-2311 fax: (303) 273-3875 email: [jcollis@mines.edu](mailto:jcollis@mines.edu)

John A. Colosi  
Department of Oceanography,  
Naval Postgraduate School  
Monterey, CA 93943  
phone: 831-656-3260, FAX: 831-656-2712,  
phone: (512) 471-4619 fax: (512) 471-1558 email: [jacolosi@nps.edu](mailto:jacolosi@nps.edu)

Steven M. Jachec  
Dept. of Naval Arch. and Ocean Engr.  
U. S. Naval Academy  
Annapolis, MD 21402  
phone: (410) 293-6429 fax: (410) 293-2219 email: [jachec@usna.edu](mailto:jachec@usna.edu)

## **LONG-TERM GOALS**

The long-term goal is to improve ocean physical state and acoustic state predictive capabilities. The goal fitting the scope of this project is the creation of physics-based, broadly applicable and portable acoustic prediction capabilities that include the effects of internal waves, surface waves, and larger scale features, with an emphasis on continental shelf and slope regions.

## **OBJECTIVES**

A fundamental objective is to improve knowledge of oceanographic processes that are known to be relevant to underwater acoustic conditions, yet are not completely understood, to shed light on predictability. Project-scale objectives are to complete targeted studies of oceanographic processes in a few regimes, accompanied by studies of acoustic propagation and scattering processes in those regimes. Internal gravity waves and other submesoscale features are of specific interest. There are many open questions regarding the processes of internal-wave formation and propagation in the presence of low-frequency large-scale ocean features, to be pursued by the basic research efforts of this project.

An additional objective is to develop improved computational tools for acoustics and for the physical processes identified by the targeted studies to be important, including work on data-driven ocean flow models. Time-stepped three-dimensional (3.5D) and true four-dimensional (4D) computational acoustic models are to be improved, as well as the methods used to couple them with ocean flow models. Fully numerical ocean flow modeling will also be improved by coupling models having nonhydrostatic pressure (NHP) physics, data-driven regional models having hydrostatic pressure (HP) physics, and surface wave models. Stochastic acoustic prediction models will be developed. The entire suite of models is to be tested for acoustic prediction effectiveness using existing data sets.

## **APPROACH**

The approach toward advancing the state of the art is to first identify acoustically relevant ocean processes, to improve environmental models of these processes, and then to use these models to study and predict the acoustic effects in detail, for comparison with existing data. The acoustical relevance of each process is best obtained with state-of-the-art acoustics research using the latest tools, with some tools in need of refinement or development, which forms part of this project. The acoustical relevancy of the processes may be such that relevancy ranking may differ from that obtained from the process relevancy rankings for ocean ecosystem, climate, or ocean biogeochemical cycle research. For example, the size, shape, direction and precise location of nonlinear internal waves is relevant because of localized acoustic effects that scale with wave size, but this level of detail is not often needed for studies of nonlinear wave impact on local ecosystems or water mass mixing. The research plan anticipates feedback, i.e. as the research evolves, goals and priorities may change.

This approach has been broken into seven tasks directed toward two goals, equivalent to the objectives listed above: (Goal #1) Development of integrated tools for joint oceanography/acoustic study and prediction, i.e. a modeling system; and (Goal #2) Develop an understanding of the physics of coastal

linear and nonlinear internal wave generation and transformation, as observed in the model, lab and field-measured features, coupled with study of acoustical propagation in these features. Verification of this understanding can be made with model/theory/data comparisons with data from ocean field studies such as the Shallow-Water 2006 experiment (SW06) east of New Jersey sponsored by ONR [1].

Achieving Goal #2 is intimately linked with the creation of modeling tools (satisfying Goal #1) because of the need to address the open questions on coastal internal wave physics, on coastal flow features, on details of NHP fluid computational modeling, and on coastal acoustic propagation effects. Each of the seven tasks is handled by a subset of the 15 total PI's. (The subsets intersect.) The project name "Integrated Ocean Dynamics and Acoustics" (IODA) was agreed on at the initial PI meeting. Here is a listing of the goals and tasks:

### **IODA project Goal 1 tasks: Modeling tools**

1. *NHP ocean model nested within data-driven HP model, tied to 4D acoustic models.*
2. *Hybrid model: Hierarchical internal-wave models nested within HP model, tied to 3.5D acoustic models. (Also called composite physics model.)*
3. *Improved 4D deterministic and stochastic acoustic modeling.*
4. *Unified waveguide model for flow and acoustics.*
5. *Integration work necessary for the above.*

### **IODA project Goal 2 tasks: Physics studies and model verification**

6. *Spatially 3D internal-wave physics studies.*
7. *Comparison of outputs and predictions with ground-truth field and lab data.*

## **WORK COMPLETED**

The end of FY 2015 corresponds to 4 years, 4 months completed in this project. Progress has been made in many areas. The completed work is grouped here by topic.

*Hybrid model development (Tasks 2 and 5, Duda, Lynch, Lin, Helfrich, Zhang):* The embedding of internal-wave propagation models in data-driven regional ocean dynamical models, for the purpose of providing input to 3.5D acoustic models for prediction testing, as well as internal-wave study, has progressed this year. This not only involves coding, but also research into how to handle detrimental effects stemming from the fact that the various fluid dynamical models have different physics approximations. A major role of the model is to test our understanding of the physics of tidally driven internal waves moving onto a continental shelf. These waves are qualitatively understood but are highly variable [2-5]. These waves are also known to have important acoustic effects [6-10, Duda et al., 2011], so knowing their physics, their predictability, and how their predictability translates to acoustic field predictability and acoustic system performance predictability is key. Arthur Newhall of WHOI is a key person in this effort.

The model extracts internal-tide modal propagation paths (ray paths) from data-driven model output, then uses a Korteweg-deVries type of nonlinear wave evolution model to compute, along the paths, linear and nonlinear internal waves at all scale that evolve from linear internal waves that are resolved by the data-driven (and tidally driven) model.

In more detail, the background state governing the internal-tide modes, and modal ray tracing, the coefficients of the wave-evolution model, and initial conditions for the wave evolution model, are taken from data-driven ocean models such as MSEAS–Primitive Equation or ROMS. The design of the model is as follows: internal wave normal-mode speeds are taken from the data-driven model, after removing internal tides; internal wave mode rays are traced (with a few options for wave-mean flow interaction complexity and source location, wave source location being one of our research topics); coefficients for the extended Korteweg-deVries equation with rotation (eKdVf, [11]) are evaluated along each ray; eKdVf is solved along each ray; the resulting high-frequency internal waves along each ray are mapped into a 3D space using interpolation schemes. 3D sound-speed fields are then ported to a 3D acoustic propagation models.

Starting at large scale and moving to small, the output of the MIT MSEAS SW06 model (see below) has been fully interfaced into the hybrid model. This model has a nested subdomain that provides well-resolved internal tides. Work at Rutgers U. (reported below) to nest, in similar fashion, an order-km scale resolving grid into the operational ESPreSSO model has progressed. The larger-scale internal waves and tides require a nested model to faithfully model internal waves and internal tides moving onto the shelf, partially because the bathymetry that vertically deflects the tidal flow to cause the waves must be accurate in the model.

Moving to nested model work, code was completed this year to (1) extract, from data-driven model output the so-called critical slope locations at the shelf break, (2) separate background conditions from high-frequency flows in the output, (3) tidally analyze the high-frequency flow to extract internal tides, (harmonic analysis), (4) beamform internal tides to initiate internal-tide ray tracing, (5) compute anisotropic internal-wave mode eigenvalues and eigenfunctions on arbitrary background flow conditions, (6) pass internal-tide initial and background conditions to the eKdVf model, (7) analyze internal-tide ray focusing, which will affect energy in the eKdVf model, and (8) build 3D sound speed fields from the modal rays, modal functions, background states, and eKdVf outputs.

The critical slope location finder (item 1) was straightforward (see Zhang and Duda, 2013 and Zhang et al., 2014 for further explanation and diagrams of the critical slope location). These are generally located just seaward of where the outer continental shelf steepens and rolls off into deep water. With weak incident internal tides, this location divides shoreward from seaward propagation of locally generated internal tides. The background condition calculation (item 2), which tracks density surface positions to compute mean density-surface heights (background state) and residual displacements (mostly but not entirely internal waves) has difficulties because of surface heat flux, precipitation and evaporation creating or destroying water of certain density classes, and because of similar density class intermittency caused by subtidal advection. This mean states and displacements are usable away from the surface, for the most part, and remaining gaps are interpolated over. The tidal analysis (item 3) is robust. The beamforming (item 4) has a subjective component at this time, which is the depth weighing of the displacement depth-time series. Figure 1 shows raw displacement inputs for analysis.

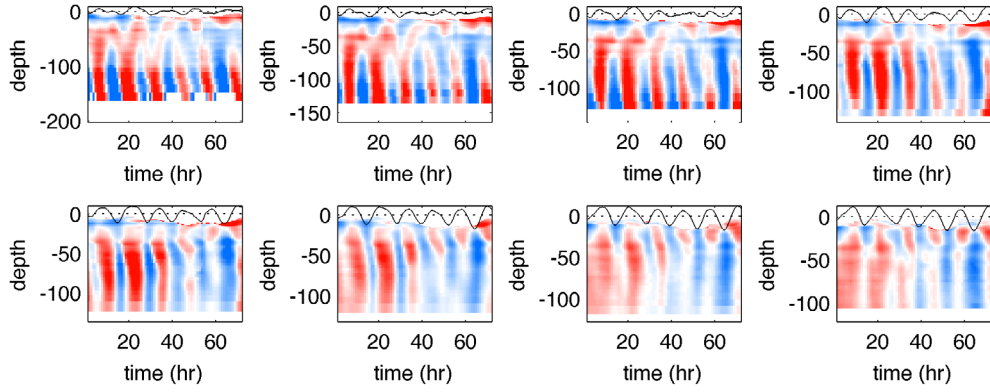


**Figure 1.** Displacement time series (72 hours) at a few internal-tide ray starting points near the continental-shelf outer edge south of Hudson Canyon are shown. Values are from the MSEAS SW06 2012 reanalysis. These must be converted to internal-wave mode-one amplitude to serve as initial conditions to drive the eKdVf along internal tide mode-one rays that will begin at the same points. The time-depth series must also be processed before beamforming (analyzing relative phase at a few sites) to give ray initial directions. The first step in the processing is tidal analysis, the next is subjective depth weighting. In the frames, red is westward current, blue eastward, with colors saturated at +/- 6 cm/s.

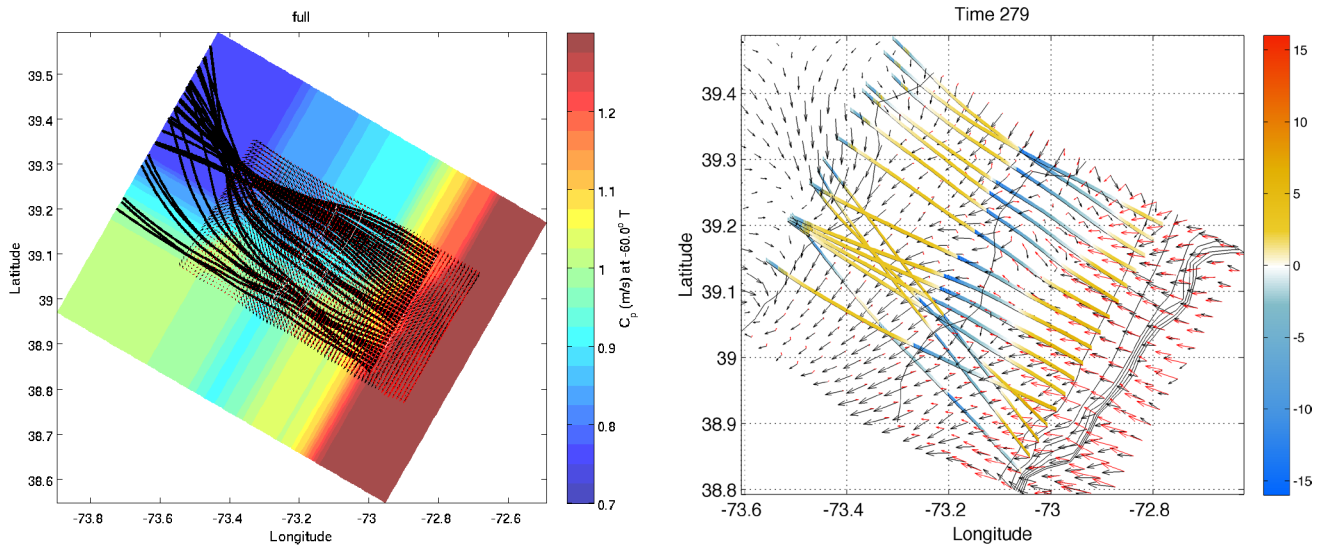


**Figure 2.** (left) Internal tide mode-one rays are drawn from starting points near the continental slope. The colors show mode-one phase speed inside the box featuring current vectors, extended outward artificially to the edges of a larger box; red marks deep water and faster waves. The rays start one-km apart in directions deduced by beamforming the tidally analyzed extracted displacements from the MSEAS 2012 SW06 reanalysis. (Run 003 time 148.) Three ray focus regions are seen. (right) Similar ray paths are shown for another computation (Test 296 time 279). Superimposed are eKdVf wave model mode-one amplitude solutions along the rays. Nonlinear internal wave packets are not highly visible here but exist at the western edges of the blue regions (down-displaced water, color scale showing meters displacement).

The internal-wave normal mode properties are found (item 5) using a generalized version of the known vertical structure equation for parallel shear flow [12]. The parallel flow condition is relaxed. The equation can be cast as a polynomial eigenvalue problem after choosing a wavenumber direction and solved for the fastest mode (mode 1). Mode-one properties are a function of wavenumber direction, thus we refer to the wave propagation as anisotropic. Ray-tracing codes were completed in prior years. The theory has been refined this year and appears in the Results section below. Figure 2 shows rays computed during two model runs. Illustrations from the ray-tracing and wave evolution computations are also shown in the Results section.

*Acoustic model development (Tasks 3 and 5; Lin, Duda, Collis, Siegmann):* Five new three-dimensional acoustic propagation codes in the MATLAB® programming environment have been completed thus far. These codes were completed in prior years and are described in the FY2013 report. Most of the codes use the now-standard wide-angle PE propagator [13,14]. Another uses the new higher-order propagator (Lin and Duda, 2012). A new code for a marching PE algorithm that handles a non-flat water surface was developed by Lin and is being interfaced to the surface wave modeling activities of Task 4.

*Ocean internal wave physics (Tasks 2 and 6; Helfrich):* The work to date has investigated the joint effects of rotation and topography. Our progress had been described in more detail in prior reports. A paper has been published, supported partially by this grant (Grimshaw et al., 2014). Future work is planned to compare South China Sea wave behavior to New Jersey Shelf wave behavior. ONR-sponsored studies have collected internal wave data at these locations, allowing data/model comparison. Tests of the ray-tracing solutions, explained in the hybrid model section, under idealized environmental conditions (stratification and topography) against high resolution, full numerical computations are planned in order to assess the potential and limitations of the ray-tracing approach.

In many situations the large-amplitude internal solitary waves that emerge from the steepening internal tide become unstable to shear instability that can lead to enhanced wave dissipation and may also affect acoustic propagation. Because the zone of low Richardson number is limited in space to near the wave crest, standard modal stability methods are not appropriate. To address this issue work has begun on using transient growth methods to assess the susceptibility of internal solitary waves to shear instability.

*Surface waves and flow (Tasks 2, 4 and 6; Lermusiaux, Yue, Liu):* Drs. Dick Yue and Yuming Liu at MIT have continued the development and verification of a robust phase-resolved simulation capability for study and prediction of the coupled dynamics of surface/internal waves with varying currents in littoral regions, by integrating a nonlinear wave simulation tool (SNOW) with an ocean-flow prediction tool (MSEAS). Large-scale simulations were performed with realistic ocean current fields (provided by MSEAS) and various wave conditions. They focused on the understanding, quantification, and characterization of the slowly-varying-current effects on nonlinear statistics of surface wave-fields and occurrence of rogue wave events in littoral regions. One new wave physics paper was published (Pan and Yue, 2015).

*Stochastic acoustic modeling (Tasks 3 and 4; Makris):* This group is continuing work towards developing determined general expressions for mean field and second moment, now including Doppler shift and spread as well as temporal coherence through fluctuating ocean. They have confirmed that transmission statistics in their 2014 Artic experiment are consistent with time-bandwidth dependent

theoretical predictions, and they have been able to numerically estimate statistical degrees of freedom for different waveguides and signal bandwidths and durations.

*Ocean modeling (Tasks 2 and 4; Lermusiaux):* The MSEAS group has continued to recalibrate the reanalysis of the SW06 experiment. One particular component has been a re-examination of the tidal input to the primitive-equation model (MSEAS PE), with a goal of improving the fidelity of the MSEAS PE tidal response as well as the resulting internal tidal fields. This re-examination includes updating the source tidal fields, the subsequent processing of the tidal forcing prior to their use in the MSEAS PE code and a re-evaluation of the MSEAS PE code itself. The dynamics of salinity intrusions in the Middle Atlantic Bight shelfbreak region was further studied, focusing on possible roles of Eady edge wave, other mixed-layer instabilities, and other submesoscale processes. We also reviewed and improved the criterion (and codes) to automatically detect the salinity intrusions. Reanalysis fields have been provided to Yuming Liu (MIT) and Nick Rypkema (MIT).

To confirm that our 2D Finite Volume (FV) nonhydrostatic model can simulate internal tide dynamics, we compared simulations of internal tides generated by tidal flow over an isolated seamount between our FV code and the MITgcm (3D, non-hydrostatic, finite volume code) and compared the results with an analytical model. The open boundary conditions on either side of the seamount were supplemented with a sponge to avoid spurious wave reflections. Stochastic Dynamically Orthogonal (DO) field equations, which are available in the 2D FV framework, were used to study the way perturbations in the density field affect the internal tides dynamics. Sigma coordinates were implemented into the 2D non-hydrostatic finite volume framework to more accurately represent complex topography and study variable generation of the internal tides.

Our 3D high-order, non-hydrostatic, finite element and projection-based ocean code that utilizes the hybridizable discontinuous Galerkin (HDG) method continued to be upgraded and verified (Ueckermann and Lermusiaux, 2015; M. P. Ueckermann, C. Mirabito, P. J. Haley Jr., and P. F. J. Lermusiaux, High order hybridizable discontinuous Galerkin projection schemes for 3D unsteady physical-biogeochemical ocean models, in preparation). The implementation of the initial conditions, boundary conditions, and source terms was adjusted to represent complex forcing using a quadrature-base scheme. Such forcing are needed for simulations with internal tides and nonlinear waves. This modification was necessary to ensure proper convergence behavior (Mirabito C., P. J. Haley Jr. and P. F. J. Lermusiaux, Verification of high order hybridizable discontinuous Galerkin-projection schemes, in preparation). Additional stability and convergence tests using this upgraded non-hydrostatic HDG code were conducted in an idealized environment, using error expansions for our spatial (prismatic element) and temporal (modified implicit-explicit Runge-Kutta) discretization for the full system. A fixed-point-like reiteration scheme was implemented for the pressure-correction projection method in rotational form for the Stokes and Navier-Stokes equations with multistep methods. This scheme was implemented and comparison tests conducted within both our non-hydrostatic, finite element code and our 2D Finite Volume code.

Several other papers are in various publication stages. Haley et al. (2015) published a methodology for creating forecast initializations which are consistent with observations, complex geometry and dynamics, and that can simulate the evolution of ocean processes without large spurious initial transients. A paper has been drafted (authors Kelly et al.) that analyzes interactions of internal tides generated at the shelfbreak front with the Gulf Stream offshore. Subramani et al. (2015) utilized the MSEAS reanalysis fields for SW06 to develop and validate a novel scheme for energy based path planning using a stochastic DO level-set optimization.

*Ocean internal tide physics (Task 6; Swinney)*: In this effort, laboratory experiments and numerical simulations of internal wave generation and propagation are conducted for tidal flow over topography, as a function of tidal frequency  $\omega$  and the vertical profiles of the buoyancy frequency,  $N(z)$ . Numerical simulations of the Navier-Stokes equations are conducted using a parallelized finite-volume based solver and run on the University of Texas Stampede supercomputer. Laboratory experiments and simulations are being conducted for various topographic arrangements.

The group has developed a method to determine, *using only velocity field data*, the time-averaged energy flux and the total radiated power for 2-dimensional internal gravity waves. This was published in Lee et al. (2014), and is described in more detail in earlier reports. The method is now available as a MATLAB code with a graphical user interface [Lee, Frank, “Internal Wave Stream Function Energy Flux and Power Calculator 5000”, <http://www.mathworks.com/matlabcentral/fileexchange/44833>].

During the last three years the relationship between boundary currents generated by tidal flow over topography and the radiated internal wave power has been examined in experiments and in simulations of tidal flow of a uniformly stratified fluid over various topographies (knife-edge, tent, Gaussian, sinusoidal). Further description of the work appears in previous year’s reports.

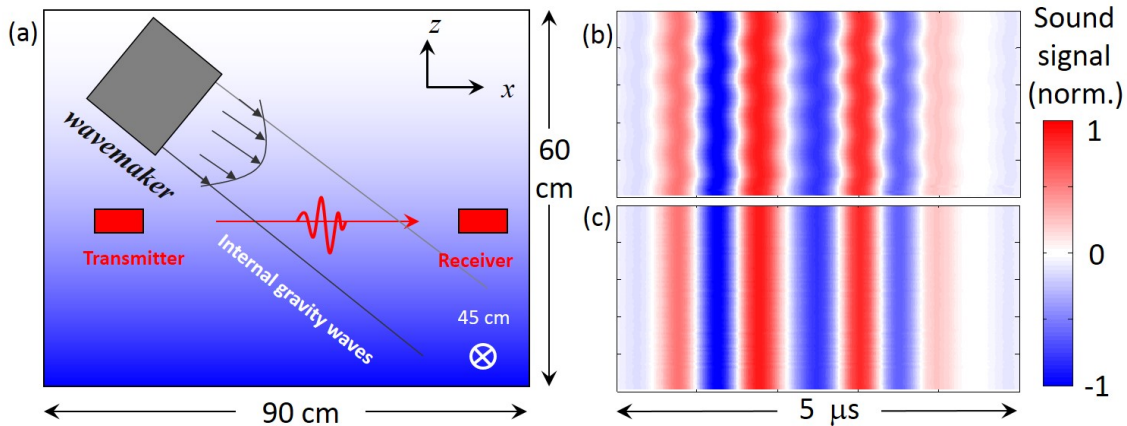


**Figure 3. (a) UT Laboratory tank with a linearly stratified fluid, designed for studies of acoustic wave propagation across an internal wave propagating at an angle with respect to the acoustic track. (b) A vertical raster of 100 successive acoustic pulses (1 MHz) that have propagated through an internal wave beam and have been detected by the receiver; the arrival time of the acoustic waves is modulated by the passage of five internal waves of period 7 seconds. (c) Same as (b), except that the internal wave generator is turned off.**

*Concurrent laboratory internal wave and acoustic measurements (Tasks 3 and 7, Swinney and Lin)*: Noise arising from internal waves generated by surface winds and random ocean topography reduces the signal-to-noise ratio of acoustic signals used in imaging and communication in the oceans. Postdoc L. Zhang of the Texas IODA group is conducting the first laboratory study of acoustic propagation in the presence of internal waves. A tank filled with a stratified fluid contains a wavemaker that generates internal waves, and an acoustic track crosses the internal wave beam, as illustrated in Figure 3. The measurements are designed to provide a benchmark for a better understanding of the influence of internal waves on 3D sound propagation in the oceans. The measurements should yield a definitive set of internal wave fields to serve as input for the “numerical tank” modeling of sound propagation with

parabolic equations by Y.-T. Lin (WHOI). Completed 3D PE modeling shows strong sound refraction good agreement with the experiment.

*Internal wave physics; Internal wave pressure, velocity, and energy flux from density perturbations (Task 6, Swinney):* In both ocean and laboratory measurements the internal wave energy flux  $J = pu$  has not been available because simultaneous measurements of the wave pressure  $p$  and velocity  $u$  are in practice not possible. However, during the current grant year the Texas IODA group has developed a method for determining the flux  $J$  from the density perturbation field alone: pressure  $p$  is deduced from the density perturbations by a Green's function technique, and velocity  $u$  is obtained by integrating the continuity equation. The method has been tested by making measurements of the density perturbation field using a schlieren method in a laboratory internal wave experiment. The results for the internal wave power deduced by applying the Green's function method to the laboratory density perturbation data are found to be in remarkable agreement (within a few percent) with results obtained in a direct numerical simulation of the Navier-Stokes equations. The Green's function method is general, and it should yield, for example, the pressure, velocity, and internal wave energy flux fields from data for density perturbations produced by lee waves and propagating vertical modes in the oceans. A manuscript is in preparation, F. M. Lee, M. R. Allshouse, P. J. Morrison, and H. L. Swinney, to be submitted to *J. Fluid Mechanics*.

*Internal wave physics; Scaling of power of internal tides on the height of the topography (Task 6, Swinney):* A study last year by the Texas IODA group revealed that the conversion of tidal energy into internal waves by tidal flow over steep random topography occurs only above a local virtual seafloor (Zhang and Swinney, 2014). During the current grant year numerical simulations have been conducted to determine how the radiated internal wave depends on the rms topographic height  $H_{rms}$  of random topography that has the spectrum of ocean topography. For weak topography the radiated power is known from linear theory to be proportional to  $H_{rms}$  squared. However, most of the internal wave power in the oceans arises from tall steep topography, and the simulations for this case indicate that the radiated internal wave power is directly proportional to  $H_{rms}$ , as shown in Figure 4. This research is now being extended to 3D random topography [F. M. Lee, M. R. Allshouse, P. J. Morrison, and H. L. Swinney]. The goal is to use topographic data from the world's oceans to develop an improved estimate of the global conversion of tidal energy into radiated internal wave power. A manuscript is under review at *Geophys. Res. Lett.*

*Internal wave physics; Material transport by boluses in shoaling internal waves (Swinney, Task 6):* Shoaling internal waves can form boluses that transport fluid and biota up a continental slope. The formation, evolution, and characterization of boluses is being examined in numerical simulations and laboratory experiments by the Texas IODA group [M. Allshouse, G. Salvador-Vieira, and H.L. Swinney]. This study is using a Lagrangian based coherent structure detection method to identify and track boluses obtained in numerical simulations and in complementary laboratory experiments. The study is examining  $\tanh(z)$  density profiles of pycnoclines with varying thickness  $h_t$ , while previous experiments and simulations focused on 2-layer systems. Results from simulations of mode 1 internal waves shoaling into pycnoclines with four different thicknesses are shown in Figure 5. In the coming grant year simulations and experiments will be conducted for pycnoclines of varying strength and thickness, and for varying angles of the continental slope. The ultimate goal is to predict the amount of fluid that is trapped and transported by boluses in ocean environments.

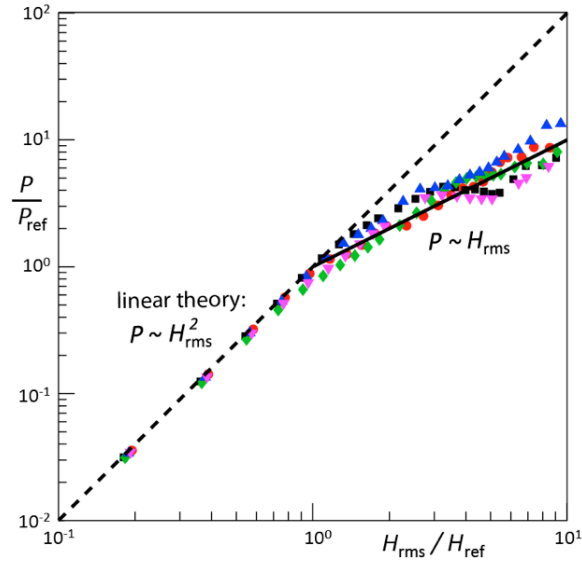


**Figure 4.** Numerical simulations of internal wave power for five different random topographies with  $H_{rms} < H_{ref}$  yield internal wave power proportional to  $H_{rms}$  squared, as predicted by linear theory. However, for tall steep topography ( $H_{rms} > H_{ref}$ ) the simulations indicate that the radiated internal wave power law depends linearly rather than quadratically on  $H_{rms}$ : the slope of the best fit log-log plot is  $\alpha = 0.96 \pm 0.07$  for  $H_{rms} > H_{ref}$ .

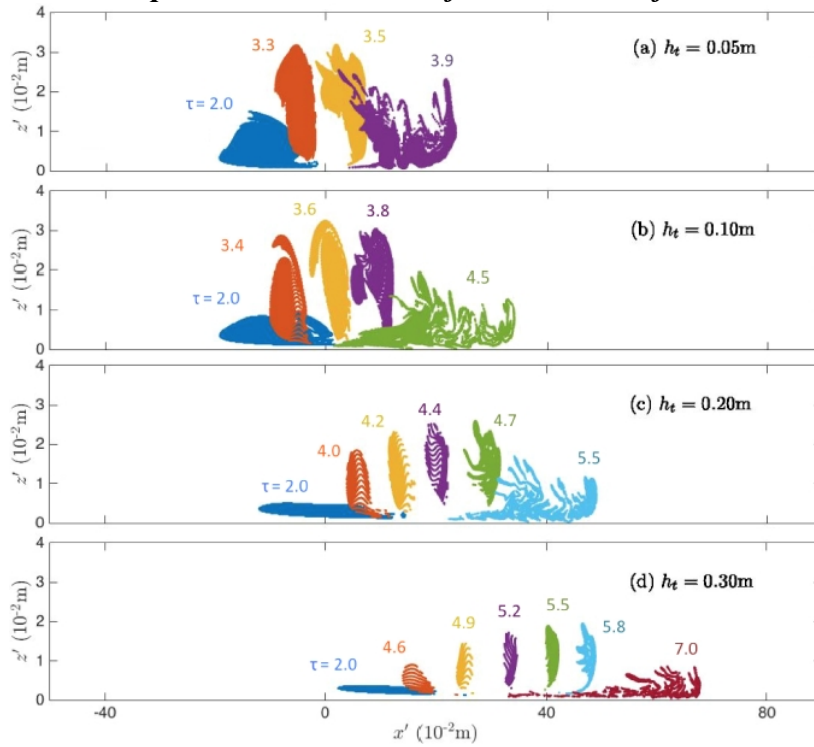


**Figure 5.** Time development and the eventual collapse of a fluid bolus formed by an internal wave shoaling up a model continental slope inclined at a 10 degree angle, for pycnoclines of increasing thickness  $h_e$ . Each panel shows the results for a numerical simulation of a single fluid bolus at different dimensionless times  $\tau$ . For thin pycnoclines such as in (a), the bolus becomes unstable and collapses before transporting material far up a slope, while for thicker pycnoclines such as in (c) and (d), a coherent bolus persists further up the slope. While thicker pycnoclines allow for longer transport times, the bolus volumes become smaller.

*Ocean internal tide generation physics (Tasks 2 and 6; Zhang and Duda):* Studies of internal tide generation made with ROMS [15] for supercritical continental slope (Zhang and Duda, 2013) and canyon geometry (Zhang et al., 2014) have shown the importance of nonlinear processes and multiple scattering processes to the resultant internal tide patterns. This work ties in well with work of the U. Texas wave physics group completed prior to this grant [16] which shows that incorrect handling of the nonlinearity is likely to cause incomplete or inadequate model results. The canyon internal-tide generation study has continued this year and now carries through to nonlinear wave formation using the hybrid model. An adjustment of the stratification to summer conditions was made to increase the nonlinear wave growth rates. A figure is shown in the Results section.

*SW06 experiment acoustic/oceanographic data analysis (Task 7; Badiy):* This group has analyzed coherence of acoustic normal modes in the presence of nonlinear internal waves on the New Jersey continental shelf. Data are from SW06. The work is directed at the project goals of evaluating modeling capabilities for the sound field spatial coherence via data/model comparison. Another goal for this work is basic understanding of the relationship between the spatial and temporal evolution of the temperature field induced by internal waves and signal fluctuations, with fluctuations characterized by temporal and spatial coherence behavior.

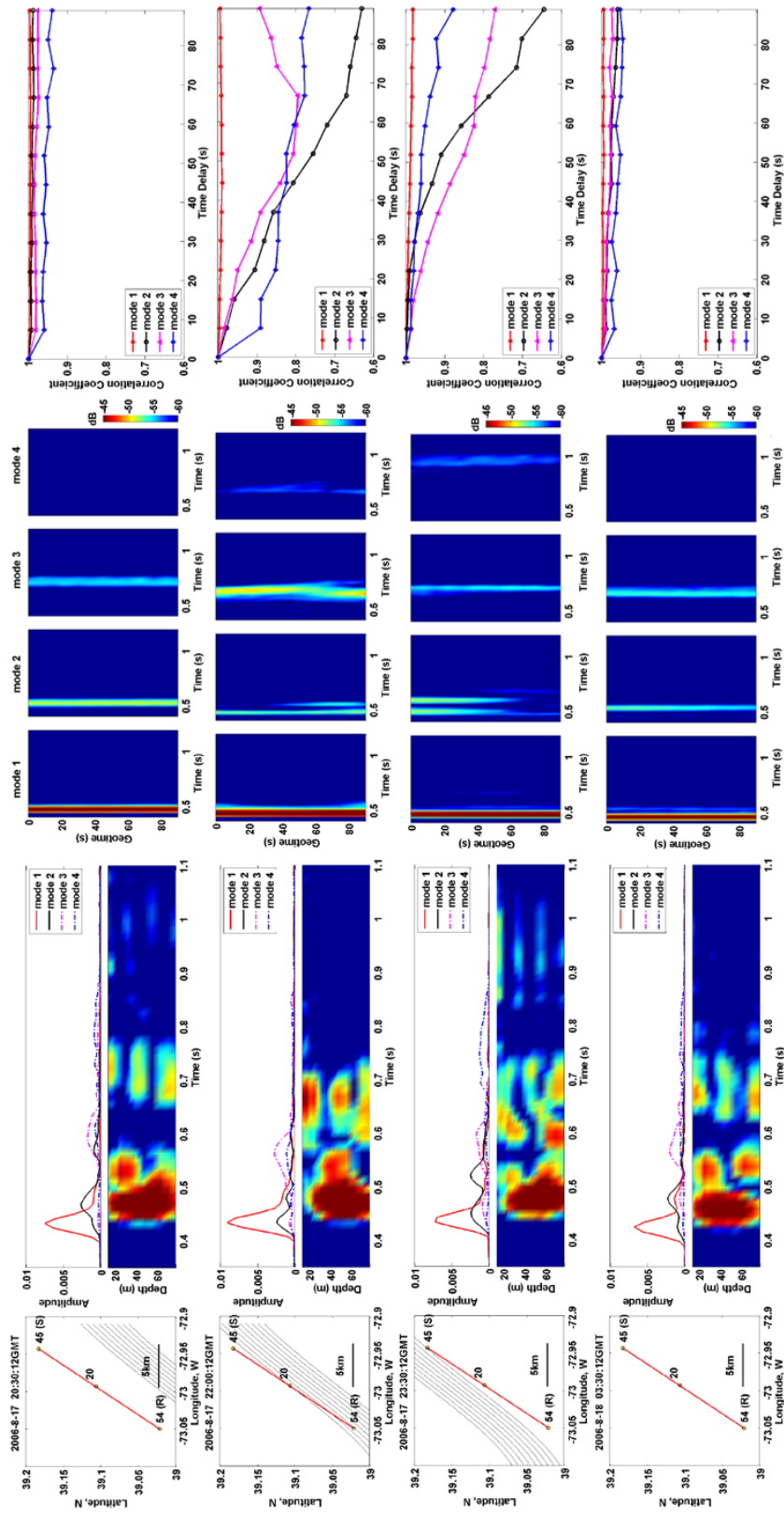


Figure 6. This set of images shows the evolution of NLIW event 48 (first column), vertical structure of received 100 Hz MSM signals (second column), decomposed modes as a function of geotime (third-sixth columns), and temporal coherence of normal modes at 100 Hz (last column).

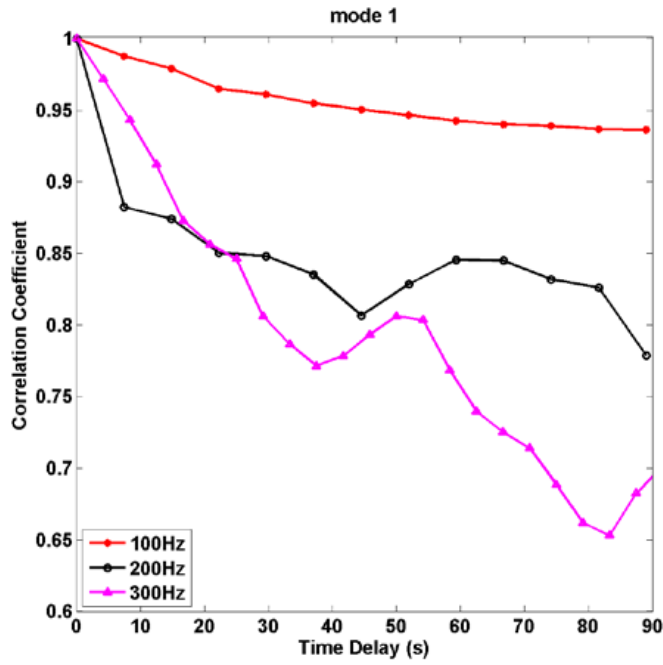


Figure 7. The short-time-lag correlation coefficient of mode 1 as a function of time delay is shown for three acoustic frequencies. The correlation coefficient is obtained by averaging the four 90-sec 100 Hz transmissions results when NLIW fronts cover the acoustic source-receiver track.

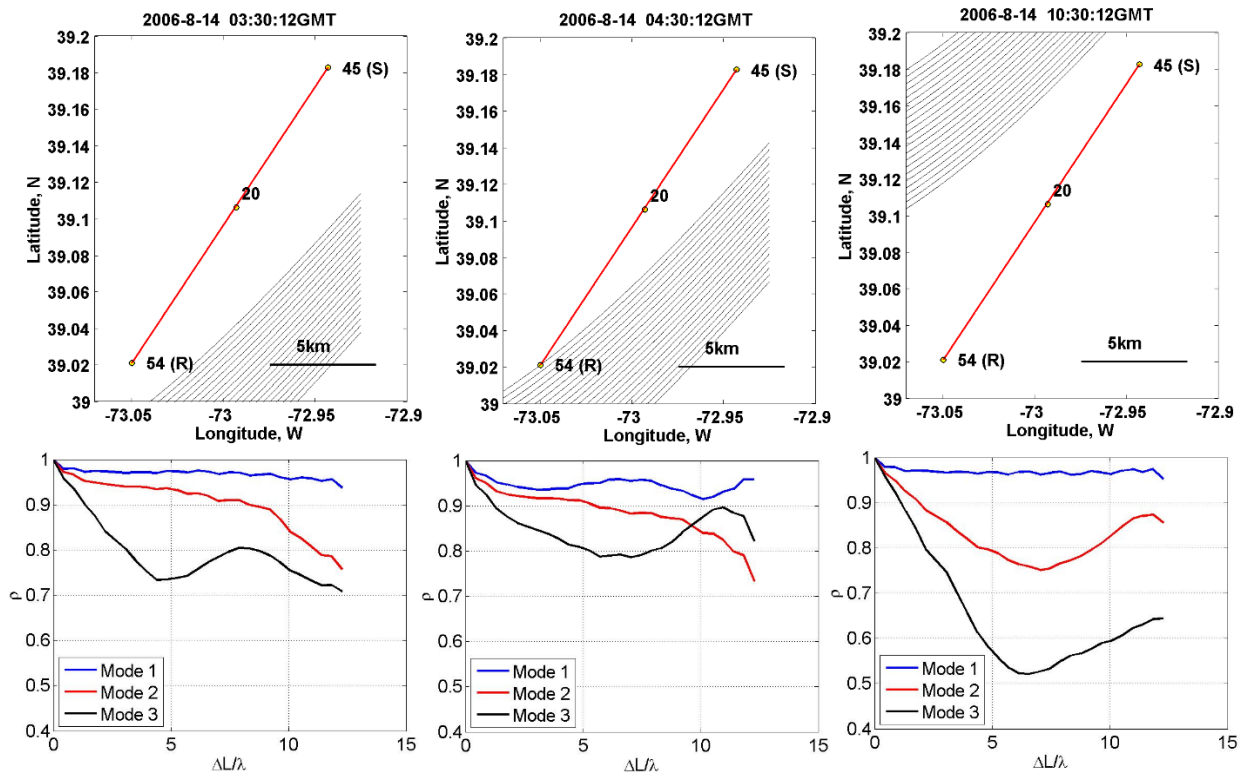


Figure 8. The picture collage shows the evolution of NLIW event 37 (upper row) and the corresponding horizontal coherence of normal modes at 100 Hz (lower row).

During SW06 the 3D temperature field for one month of nonlinear internal wave (NLIW) events has been reconstructed. The IW events, having an angle between the acoustic track and IW fronts varying from -8 deg. to 83 deg., were measured as acoustic signals were concurrently transmitted from fixed sources at an along-shelf distance of about 20 km with frequencies at 87.5–112.5 Hz (m-sequence), 175–225 Hz (m-sequence), 270–330 Hz (chirp), respectively. The acoustic signals were recorded by an L-shaped hydrophone array moored inside the area with NLIW measurements. In this research, these internal wave events have been used to investigate their effects on the coherence of acoustic normal modes decomposed from the measured acoustic field. The coherence of sound field is obtained as a function of frequencies for different NLIW events.

The temporal coherence of normal modes is illustrated in Figures 6 and 7. Figure 1 shows the position of one NLIW over time, along with acoustic normal mode statistics. Figure 2 shows acoustic mode-one coherence versus time for three frequencies. This NLIW has small angle between the acoustic track and the internal wave crests. Four conclusions for this NLIW/acoustics interaction can be drawn from the figures:

- (1) Selected modes start to decorrelate when the NLIW is approaching the acoustic source-receiver track;
- (2) Modes are decorrelated faster when the NLIW cover the acoustic source-receiver track;
- (3) Background internal waves or the tail of the NLIW shows effect on selected modes; and
- (4) Modes start to re-correlate after the NLIW fronts pass the acoustic source-receiver track.

Figure 8 shows the horizontal coherence of individual normal modes obtained before, at the onset, and after one NLIW event during SW06.

*Acoustic regimes and feature models (Tasks 2 and 3; Lynch and Colosi):* Work has been done on developing simple analytical expressions for how various important acoustic quantities (horizontal array coherence length, transmission loss, scintillation index) depend on the parameters of the internal waves (and other coastal processes, such as fronts, eddies, spice.) With such expressions, one can rapidly calculate acoustic parameter dependencies on ocean model parameters. Given tolerance specification for error in the acoustic quantities, the models can be used to estimate how much error can be tolerated in the feature model parameters or ocean dynamical model fields. The analytic model results may allow better interpretation of the physics of the more complicated models, and may provide a simple way to predict acoustically useful things like frequency dependence, and source to receiver geometry dependence. This approach was described in a general-audience paper published last year (Lynch et al., 2014).

*Nested ocean modeling (Task 2; Zhang, Wilken):* Both the fully numerical (Task 1) and hybrid (Task 2) coastal internal wave modeling and analysis efforts require broad-scale ocean fields best obtained from data-driven modeling. The operational data-driven model for the northeastern US coast developed at Rutgers, the ESPreSSO model (<http://www.myroms.org/espresso/>), was evaluated against independent CTD and glider data over the past years. The model has very good bias performance compared to other models for the region, showing that the anti-bias methods are effective. The model also has good dynamical feature accuracy, showing low centered RMS difference values in various seasons and subsets of the domain. Work has proceeded to drive two-way nested subdomains within the model. These would have coverage and resolution required to effectively model internal tides and internal waves, for the hierarchical hybrid internal wave model and linked acoustic model. Figure 9 shows model fields and in particular an (interfacial mode-one) internal tide wave in the SW06 area.

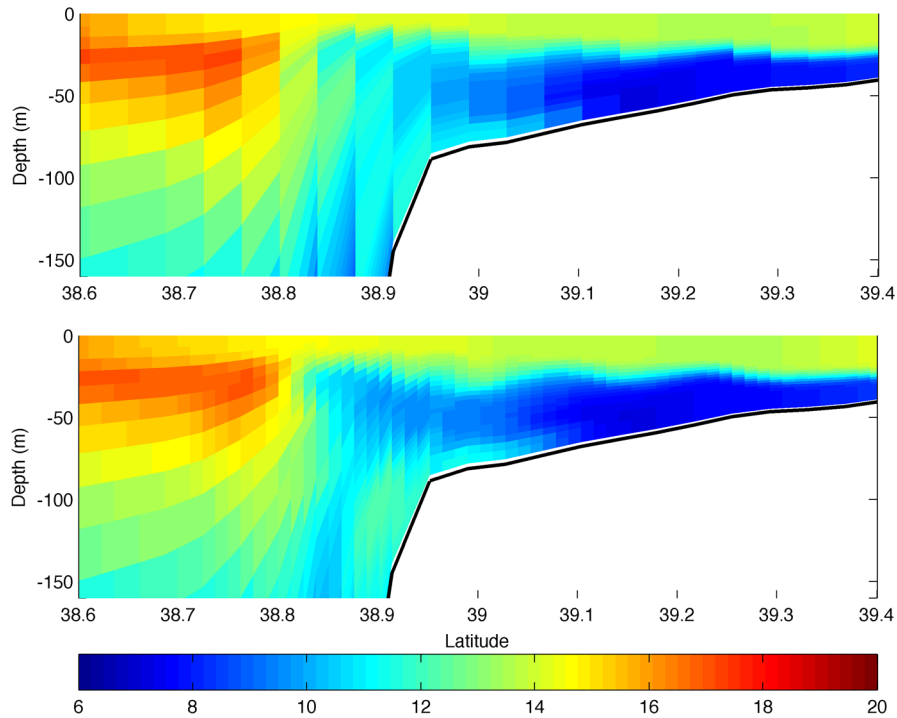


**Figure 9.** Upslope/across-shelf temperature cross sections are shown for the data-driven ESPreSSO model (top) and for a high-resolution module nested within ESPreSSO. The difference in the detail of the internal tides is evident. (Transect time 30-May-2013 01:00:00. The transect runs through the SW06 central mooring area)

## RESULTS

A few highlighted project results for this year are presented. Specific task results such as those shown here have enabled us to come close to our goal (desired result) of being able to make reliable predictions of eddy features and wave features in chosen areas and thus make reliable acoustically related calculations. A similar desired result is to understand the limits of prediction.

*Ocean modeling (Lermusiaux):* A main result from the updated tidal processing is to ensure that the tidal input fields satisfy, as much as possible, the same (nonlinear) dynamics as the MSEAS PE fields. This improved the ability of the PE to reproduce the input tidal forcing. In particular, the MSEAS PE uses a quadratic formulation for the bottom drag; as a result, an iterated scheme was introduced into the linear tidal model to implement a quadratic bottom drag. For the study of the dynamics of salty intrusions, a better detection scheme was obtained. Specifically, replacing the requirement that  $S_{max} > 33.4$  psu with the requirement that the subsurface maximum salinity needs to exceed the minimum salinity beneath it by 0.15 psu reduced false positives. An example of the improved estimate of the intrusion for 24 Sep 2006, along with several of the dynamical fields along the intrusion are shown in Figure 10.

The FV code was tested with an idealized flow past a seamount (Figure 11). The internal wave field from the FV code agreed very well with results from the MITgcm (3% relative difference) and with theoretical predictions (2.5% relative error). We found that a sigma coordinate system will reduce the numerical artifacts near the generation site, compared to a Cartesian coordinate grid.

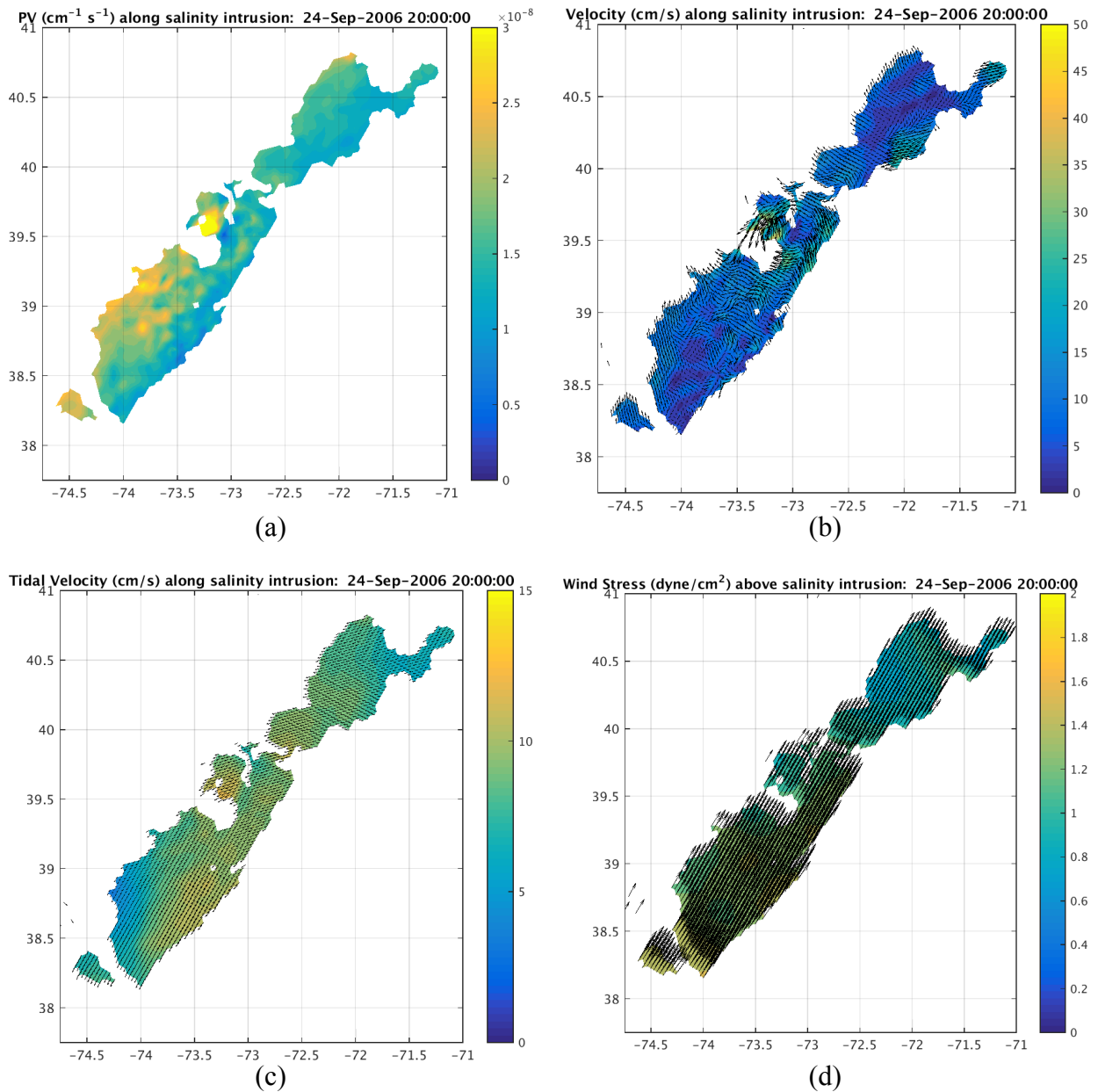


**Figure 10. Examining the dynamics of the salinity intrusions on Sep. 24, 2006. (a) potential vorticity, (b) total velocity, (c) tidal velocity and (d) wind stress along the intrusion.**

Two key results for the HDG finite element code were derived (Ueckermann and Lermusiaux, 2015). First, the HDG edge-space updates derived for the HDG rotational correction in the projection method are crucial to obtain stable 3D dynamical behavior in non-hydrostatic regimes, and are desirable for increased model fidelity in the presence of internal waves. Second, the derivation of the final recombination step for our implicit-explicit Runge-Kutta (IMEX-RK) time-integration scheme was also useful. For the tests using the reiteration scheme, the results indicate that a gain in the temporal convergence order can be achieved in some cases. The scheme helped increase the accuracy of the projection method and the resulting velocity field was both divergence free and satisfied the tangential boundary condition everywhere.

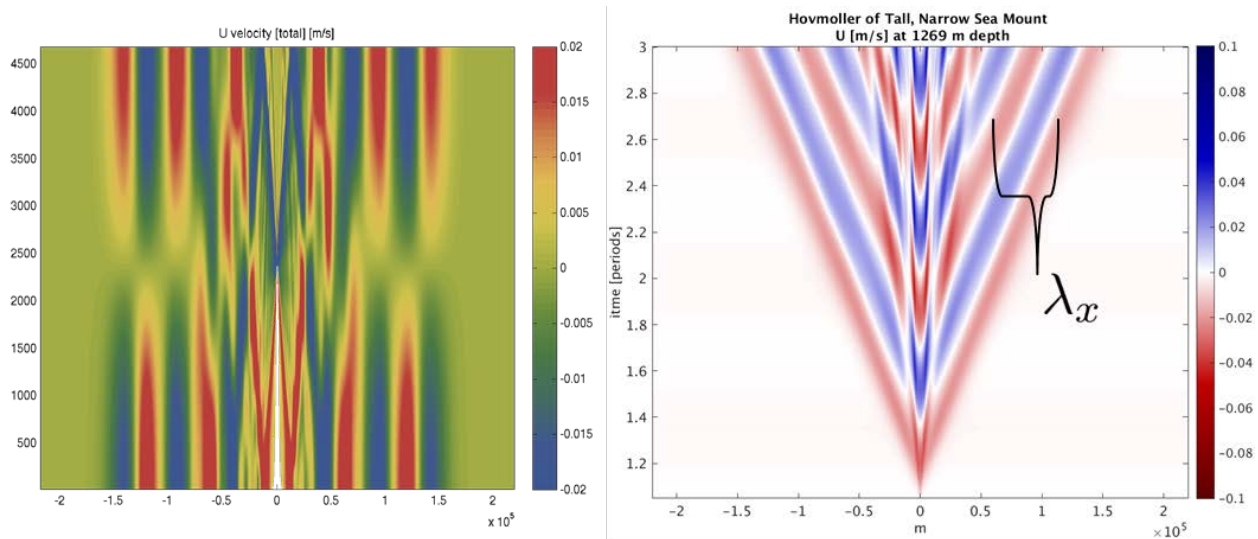


**Figure 11. Simulation of internal tides generated by linearly stratified flow over an isolated seamount and (right) a Hovmoller plot created from the timeseries of this simulation.**

A key result of Haley et al. (2015) was that our initialization methodology corrects transports, satisfies boundary conditions and redirects currents. Hindcasts from our initializations were shown to have smaller errors than hindcasts from other, common initialization strategies. A key finding of Subramani et al. (2015) was that the energy-optimal path planning methodology could save as much as 25% of the energy expenditure for an AUV in the shallow-water O6 region. Such a saving could have an important impact on future coupled ocean-acoustics studies. A paper in preparation (S. M. Kelly, P. F. J. Lermusiaux and P. J. Haley Jr., Analysis of internal-tide interactions with subtidal flows in the Middle 2 Atlantic Bight using a primitive equation model) shows that anomalous regions of mode-1 internal tide energy-flux divergence can be explained by the mean-flow terms in the mode-1 energy balance.

*Hybrid modeling (Duda, Lin, Helfrich, Zhang, Lynch):* A dimensionful version of the solver for the regularized version of the extended Korteweg-deVries equation with rotation (eKdVf, [10]) was developed prior to this year and is embedded in our suite of codes. The eKdVf code is a wave evolution model for nonlinear and nonhydrostatic waves or other features, such as bores, that fit within an ocean waveguide normal-mode framework. The new version runs quickly and reliably. Precise behaviors of the quadratic-nonlinear version of this (KdVf) are the subject of a published paper (Grimshaw et al., 2014). Figure 2 (right-hand side) shows nonlinear internal wave heights along the rays.

By finding rays near a reference point, an internal-wave time series prediction can be computed by adding eKdVf output. Waves along intersecting rays are inferred to not deform while interacting. Figure 12 shows the result for SW06 mooring SW30 location, for the early Test-296 case. In this model configuration, the nonlinear waves traveling northwestward to this site do not form in the model as rapidly as in nature, needing to travel over 7 km further (about 2 hours) to form waves similar to those measured. The times of wave packets do not match well at this stage of modeling. Note that internal tide rays can cross, giving multiple slightly lagged wave packet arrivals at a site. These are treated independently at this time and are drawn independently in Figure 12.

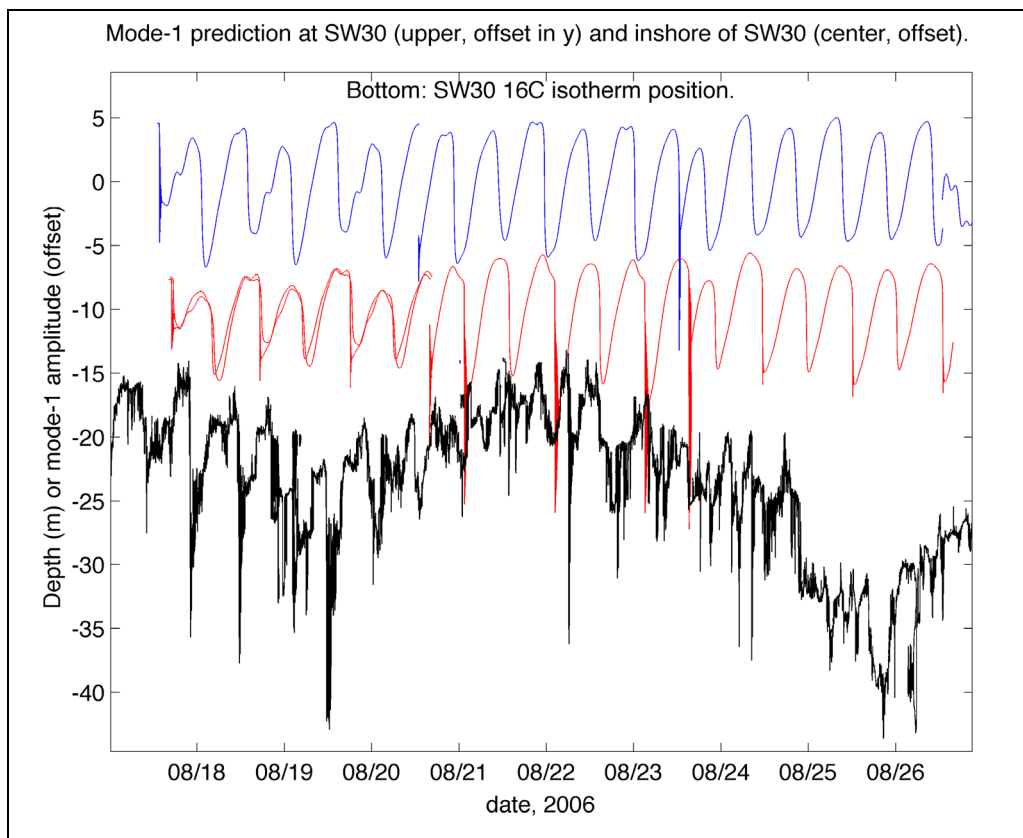


**Figure 12. Mode-one internal wave amplitude predictions from the hierarchical internal wave model are compared with data from the SW06 experiment mooring SW30. The bottom trace in black is the SW06 16°C isotherm height, which shows subtidal features that are not shown for the wave model. The top trace is the wave model prediction for that site. The middle trace is for site about 7.7 km shoreward, about two hours later in the life cycle of a local tide-generated internal wave.**

The final illustration of the model output is shown in Figure 13. Here, a regional model field similar to that used in our canyon internal wave study (Zhang et al., 2014) was input to the hybrid model. The model yielded mode-one internal tide rays moving to the right of the canyon (looking upslope), and formed strong NLIW on that side of the canyon, as seen in the reproduces SAR image. The model canyon is generic and the model is not intended to exactly imitate behavior at the imaged Hudson canyon.

The first end-to-end calculation from the hybrid model, yielding acoustic field properties within nonlinear internal waves computed with the data-driven regional model/internal tide ray/eKdVf wave evolution model/3D interpolation flow-model hierarchy and a linked 3D PE model were completed last year and a figure appears in last year's report.

*Internal wave physics: Geometrical (ray) propagation of internal wave modes (Lin):* Internal wave modes in vertically sheared currents that also vary laterally have anisotropic phase speeds when viewed in a motionless reference frame where the wave frequency is constant. One way to study this mode propagation in this situation is using ray-tracing in the “geometrical regime”. New ray-tracing equations have been derived using a Hamiltonian formulation. The governing equation is the 2D anisotropic Helmholtz equation,

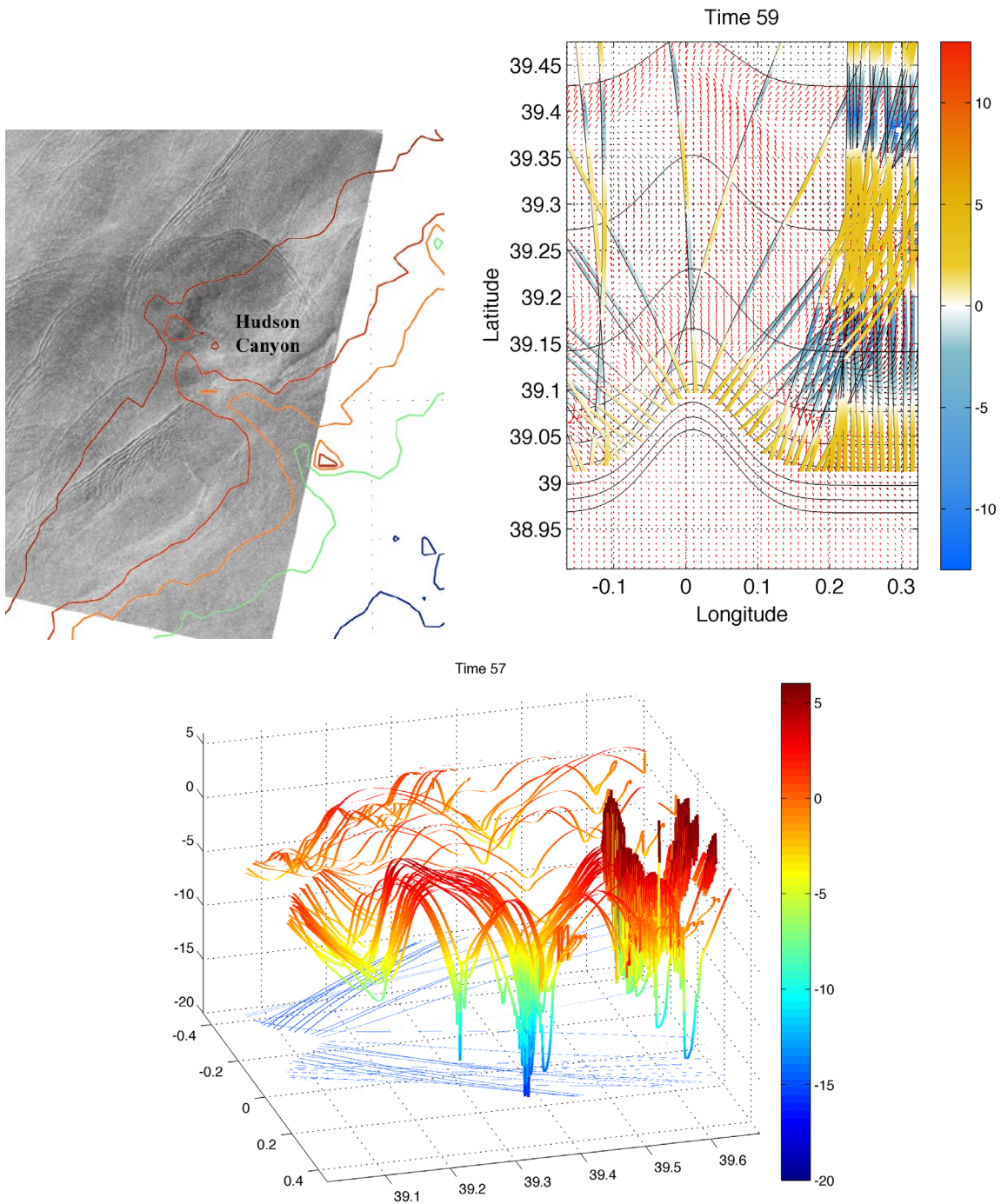


**Figure 13. (left) An image extracted from Jackson [2] showing, in satellite synthetic aperture radar (SAR) data, internal waves traveling northward, which is to the right of Hudson Canyon when looking up the canyon. (Top right) Internal tide mode-one rays are plotted; bathymetry is contoured; mean currents induced by drag and mixing are shown with arrows. Colors along the rays indicate mode-one wave displacements from the wave evolution model. (lower) The mode-one wave displacements along the rays from the wave evolution model are drawn in 3D.**

$$\frac{\partial^2 A}{\partial x^2} + \frac{\partial^2 A}{\partial y^2} + \frac{\omega^2}{c^2(x, y, \alpha, \omega)} A = 0$$

where  $A$  is the wave field variable,  $(x, y)$  is a 2D position vector,  $\omega$  is the wave frequency,  $c$  is the anisotropic phase speed, and  $\alpha$  is the direction of the vector normal to the phase front at  $(x, y)$ . To derive the ray-tracing formula, let  $A$  take the form  $\hat{A}(x, y)\exp[i\omega\Gamma(x, y)]$ , and making the WKB approximation we find the following Hamiltonian function that is preserved along energy paths (rays):

$$H = \mathbf{p}_x^2 + \mathbf{p}_y^2 - c^{-2}$$

Here,  $\mathbf{p} = (p_x, p_y)$  is the spatial gradient vector of the phase function  $\Gamma$  so that  $\alpha$  is  $\tan^{-1}(p_y/p_x)$ . The canonical coordinates are ray position components ( $x$  and  $y$ ) and phase gradient components.

Hamilton's equations for the path along which the Hamiltonian is preserved can then be cast into this form which uses the variable wave slowness  $S = 1/c$  :

$$\left\{ \begin{array}{l} \frac{dx}{ds} = \left[ S^2 + \left( \frac{\partial S}{\partial \theta} \Big|_{\theta=\alpha} \right)^2 \right]^{-1/2} \left( \cos \alpha \cdot S + \sin \alpha \cdot \frac{\partial S}{\partial \theta} \Big|_{\theta=\alpha} \right) \\ \frac{dy}{ds} = \left[ S^2 + \left( \frac{\partial S}{\partial \theta} \Big|_{\theta=\alpha} \right)^2 \right]^{-1/2} \left( \sin \alpha \cdot S - \cos \alpha \cdot \frac{\partial S}{\partial \theta} \Big|_{\theta=\alpha} \right) \\ \frac{dp_x}{ds} = \left[ S^2 + \left( \frac{\partial S}{\partial \theta} \Big|_{\theta=\alpha} \right)^2 \right]^{-1/2} S \frac{\partial S}{\partial x} \\ \frac{dp_y}{ds} = \left[ S^2 + \left( \frac{\partial S}{\partial \theta} \Big|_{\theta=\alpha} \right)^2 \right]^{-1/2} S \frac{\partial S}{\partial y} \\ \alpha = \tan^{-1}(p_y/p_x) \end{array} \right.$$

Here,  $s$  is the arc length along a ray, having components  $dx$  and  $dy$ . The azimuthal gradient of slowness  $\partial S/\partial \theta$  associates the anisotropy of phase speed with the ray trajectories. This set of first-order differential equations with respect to  $s$  can be solved by giving a set of initial conditions for the ray position  $(x_0, y_0)$  and ray angle  $\beta_0 = \tan^{-1}(dy/dx|_{s=s_0})$ , first requiring the initial angle  $\alpha_0$  of the phase front which is obtained by solving this equation stemming from the definition of group velocity,

$$\tan \beta_0 = \frac{\tan \alpha_0 \cdot S + \partial S/\partial \theta|_{\theta=\alpha_0}}{S - \tan \alpha_0 \cdot \partial S/\partial \theta|_{\theta=\alpha_0}}$$

The ray angle  $\beta = \tan^{-1}(dy/dx)$  is parallel to the group velocity vector  $(\partial \omega / \partial k_x, \partial \omega / \partial k_y)$  where wavenumber vector  $\mathbf{k}$  is parallel to vector  $\mathbf{p}$ . These equations outline a general theory for propagation of waves with anisotropic refractive index. Internal wave modal waves in the ocean in the presence of arbitrary vertically sheared currents (including geostrophic currents) are waves of this type.

*Internal tide generation (Zhang and Duda):* The idea that nonlinear physics determines the energy ultimately found in internal tides at supercritically steep slopes, and the internal tide phase, is supported by evidence in the Zhang and Duda 2013 paper. This means that linear models of internal tide generation, which are common, may be very good for some purposes, but may not be suited for detailed prediction of internal tides and the packets of nonlinear waves that they can spawn. That being said, a linearized (but multiple-scatter) internal tide model has been successfully used to explain horizontal beam patterns of internal tides generated in canyons in fully nonlinear ROMS simulations (Zhang et al., 2014), although the model may not be useful for predicting existence and phase (arrival time) of the nonlinear wave packets found to influence acoustics. Further discussion of this can be found in last year's report.

## **IMPACT/APPLICATIONS**

The creation of a modeling suite that includes submesoscale features as well as data assimilation is expected to be a valuable asset to apply in numerous ocean regions. Identification of acoustic propagation and noise field features that are controlled by local oceanographic processes may allow exploitation or mitigation of the effects.

An MIT analytical acoustic model, described in earlier years, enables prediction of the temporal coherence time scale and Doppler-shift of acoustic field fluctuations after propagating through a fluctuating ocean waveguide with random 3D surface and internal gravity waves.

## **TRANSITIONS**

The MSEAS random noise ocean process models from MIT are being transitioned to NRL. The procedure of inserting the virtual seafloor internal-tide parameterization into global ocean and global climate models is being investigated by the NOAA Geophysical Fluid Dynamics Laboratory.

## **RELATED PROJECTS**

There are many closely related projects among the many co-PI's. Some of the acoustics PI's have ONR grants related to shallow-water acoustics. Several of the ocean dynamical modeling PI's have closely related projects on data assimilation, dynamical processes, and/or model development funded by both ONR and the National Science Foundation.

## **REFERENCES**

- [1] Tang, D. J., J. N. Moum, J. F. Lynch, P. Abbot, R. Chapman, P. Dahl, T. Duda, G. Gawarkiewicz, S. Glenn, J. A. Goff, H. Graber, J. Kemp, A. Maffei, J. Nash and A. Newhall, Shallow Water 2006: a joint acoustic propagation/nonlinear internal wave physics experiment, *Oceanography*, 20(4), 156-167, 2007.
- [2] Jackson, C. R., "*An Atlas of Internal Solitary-Like Waves and Their Properties, 2nd ed.*," Global Ocean Associates, Alexandria, VA, [http://www.internalwaveatlas.com/Atlas2\\_index.html](http://www.internalwaveatlas.com/Atlas2_index.html), 2004.
- [3] Duda, T. F., J. F. Lynch, J. D. Irish, R. C. Beardsley, S. R. Ramp, C.-S. Chiu, T. Y. Tang and Y. J. Yang, Internal tide and nonlinear internal wave behavior at the continental slope in the northern South China Sea, *IEEE J. Oceanic Eng.*, 29, 1105-1130, 2004.

- [4] Shroyer, E. L., J. N. Moum, and J. D. Nash, Energy transformations and dissipation of nonlinear internal waves over New Jersey's continental shelf, *Nonlin. Processes Geophys.* 17, 345–360, 2010.
- [5] Shroyer, E. L., J. N. Moum, and J.D. Nash, Nonlinear internal waves over New Jersey's continental shelf, *J. Geophys. Res., Oceans*, 116. C3, 2011.
- [6] Badiey, M., B. G. Katsnelson, J. F. Lynch, S. Pereselkov, and W. L. Siegmann, “Measurement and modeling of three-dimensional sound intensity variations due to shallow-water internal waves,” *J. Acoust. Soc. Am.* 117, 613–625, 2005
- [7] Duda, T. F., J. M. Collis, Y.-T. Lin, A. E. Newhall, J. F. Lynch and H. A. DeFerrari, Horizontal coherence of low-frequency fixed-path sound in a continental shelf region with internal-wave activity, *J. Acoust. Soc. Am.*, 131, 1782-1797, 2012.
- [8] Lynch, J. F., Y.-T. Lin, T. F. Duda and A. E. Newhall, Acoustic ducting, reflection, refraction, and dispersion by curved nonlinear internal waves in shallow water, *IEEE J. Oceanic Eng.*, 35, 12-27, 2010.
- [9] Lin, Y.-T., T. F. Duda, and J. F. Lynch, Acoustic mode radiation from the termination of a truncated nonlinear internal gravity wave duct in a shallow ocean area, *J. Acoust. Soc. Am.*, 126, 1752-1765, 2009.
- [10] Badiey, M., B. G. Katsnelson, Y.-T. Lin, and J.F. Lynch, Acoustic multipath arrivals in the horizontal plane due to approaching nonlinear internal waves., *J Acoust. Soc. Am.* 129, EL141-EL147, 2011.
- [11] Holloway, P. E., E. Pelinovsky, and T. Talipova, A generalized Korteweg-de Vries model of internal tide transformation in the coastal zone, *J. Geophys. Res.*, 104, 18,333-18,350, 1999.
- [12] Jones, W. L., Propagation of internal gravity waves in fluids with shear flow and rotation. *J. Fluid Mech.* 30, 439–448, 1967.
- [13] Thomson, D. J. and N. R. Chapman, N. R., A wide-angle split-step algorithm for the parabolic equation, *J. Acoust. Soc. Am.*, 74, 1848-1854, 1983.
- [14] Feit, M. D., and J. A. Fleck, Jr., Light propagation in graded-index fibers, *Appl. Opt.*, 17, 3990-3998, 1978.
- [15] Shchepetkin, A. F. and J. C. McWilliams, Computational kernel algorithms for fine-scale, multiprocess, long-term oceanic simulations. *Handbook of Numerical Analysis. XIV: Computational Methods for the Ocean and the Atmosphere*, P. G. Ciarlet, T. Temam, and J. Tribbia, Eds., Elsevier Science, 119-182, 2008.
- [16] King, B., H. P. Zhang, and H. L. Swinney, Tidal flow over three-dimensional topography generates out-of-forcing-plane harmonics, *Geophys. Res. Lett.*, 37, L14606, 2010.

## PUBLICATIONS

Badiey, M., L. Wan and A. Song, Three-dimensional mapping of internal waves during the Shallow Water 2006 experiment, *J. Acoust. Soc. Am.*, 134, EL7-EL13, [dx.doi.org/10.1121/1.4804945](https://doi.org/10.1121/1.4804945), 2013. [published, refereed]

- Colin, M. E. G. D., T. F. Duda, L. A. te Raa, T. van Zon, P. J. Haley Jr., P. F. J. Lermusiaux, W. G. Leslie, C. Mirabito, F. P. A. Lam, A. E. Newhall, Y.-T. Lin, and J. F. Lynch, Time-evolving acoustic propagation modeling in a complex ocean environment, in Proceedings of Oceans '13 (Bergen) Conference, IEEE/MTS, 2013. [published, not refereed]
- Dettner, A., H. L. Swinney, and M. S. Paoletti, Internal wave and boundary current generation by tidal flow over topography, *Physics of Fluids*, 25, 1-15, [doi.org/10.1063/1.4826984](https://doi.org/10.1063/1.4826984), 2013. [published refereed]
- Duda, T. F., Theory and observation of anisotropic and episodic internal wave effects on 100-400 Hz sound, in Proceedings of the International Conference and Exhibition on Underwater Acoustic Measurements: Technologies and Results, Kos, Greece, pp. 999-1006, 2011. [published, not refereed]
- Duda, T. F., Plenary presentation: Identifying and meeting new challenges in shallow-water acoustics, in Proceedings of Acoustics 2013 (AAS2013), Science, Technology and Amenity, Australian Acoustical Society, 2013. [published, not refereed]
- Duda, T. F., Y.-T. Lin and D. B. Reeder, Observationally constrained modeling of sound in curved ocean internal waves: Examination of deep ducting and surface ducting at short range, *J. Acoust. Soc. Am.*, 130, 1173-1187, [dx.doi.org/10.1121/1.3605565](https://dx.doi.org/10.1121/1.3605565), 2011. [published, refereed]
- Duda, T., Y.-T. Lin and B. D. Cornuelle, Scales of time and space variability of sound fields reflected obliquely from underwater slopes, *Proc. Meet. Acoust.*, 19, 070025, 2013. [published, not refereed]
- Duda, T. F., Y.-T. Lin, A. E. Newhall, K. R. Helfrich, W. G. Zhang, M. Badiy, P. F. J. Lermusiaux, J. A. Colosi and J. F. Lynch, The "Integrated Ocean Dynamics and Acoustics" (IODA) hybrid modeling effort, in Proceedings of the 2nd International Underwater Acoustics Conference, Rhodes, Greece, 2014. [published, not refereed]
- Duda, T. F., W. G. Zhang, and Y.-T.-Lin, Studies of internal tide generation at a slope with nonlinear and linearized simulations: Dynamics and implications for ocean acoustics, in Proceedings of Oceans '12 (Hampton Roads) conference, MTS/IEEE, 2012. [published, not refereed]
- Duda, T. F., W. G. Zhang, K. R. Helfrich, A. E. Newhall, Y.-T. Lin, and J. F. Lynch, Issues and progress in the prediction of ocean submesoscale features and internal waves, in Proceedings of Oceans '14 (St. John's) conference, IEEE/MTS, 2014. (9 pp.) [published, not refereed]
- Emerson, C., J. F. Lynch, P. Abbot, Y.-T. Lin, T. F. Duda, G. G. Gawarkiewicz, and C.-F. Chen, Acoustic propagation uncertainty and probabilistic prediction of sonar system performance in the southern East China Sea continental shelf and shelfbreak environments, *IEEE J. Oceanic Eng.*, 2015. [published, refereed]
- Gong, Z., T. Chen, P. Ratilal, and N. C. Makris, Temporal coherence of the acoustic field forward propagated through a continental shelf with random internal waves, *J. Acoust. Soc. Am.*, 134, 3476-3485, 2013. [published, refereed]
- Grimshaw, R., C. Guo, K. Helfrich, and V. Vlasenko, Combined effect of rotation and topography on shoaling oceanic internal solitary waves, *J. Phys. Oceanogr.*, 44, 1116-1132, 2014. [published, refereed]
- Haley, P. J. Jr., A. Agarwal, and P. F. J. Lermusiaux, Optimizing velocities and transports for complex coastal regions and archipelago. *Ocean Modeling*, 89, 1-28, 2015. [published, refereed]

- Kiara, A., K. Hendrickson and D. K. P. Yue, SPH for incompressible free-surface flows. Part II: Performance of a modified SPH method, *Computers and Fluids*, 86, 510-536, [dx.doi.org/10.1016/j.compfluid.2013.07.016](http://dx.doi.org/10.1016/j.compfluid.2013.07.016), 2013. [published, refereed]
- King, B., M. Stone, H. P. Zhang, T. Gerkema, M. Marder, R. B. Scott, and H. L. Swinney, Buoyancy frequency profiles and internal semidiurnal tide turning depths in the oceans, *J. Geophys. Res. (Oceans)* 117, C04008, [dx.doi.org/10.1029/2011JC007681](http://dx.doi.org/10.1029/2011JC007681), 2012. [published, refereed]
- Lee, F. M., M. S. Paoletti, H. L. Swinney, and P. J. Morrison. Experimental determination of radiated wave power without pressure field data, *Physics of Fluids*, 26, 046606, doi: 10.1063/1.4871808, 2014. [published, refereed]
- Lin, Y.-T. and T. F. Duda, A higher-order split-step Fourier parabolic-equation sound propagation solution scheme, *J. Acoust. Soc. Am.*, 132, EL61-EL67, 2012. [published, refereed]
- Lin, Y.-T., J. M. Collis, and T. F. Duda, A three-dimensional parabolic equation model of sound propagation using higher-order operator splitting and Padé approximants, *J. Acoust. Soc. Am.*, 132, EL364-370, [dx.doi.org/10.1121/1.4754421](http://dx.doi.org/10.1121/1.4754421), 2012. [published, refereed]
- Lin, Y.-T., T. F. Duda, and A. E. Newhall, Three-dimensional sound propagation models using the parabolic-equation approximation and the split-step Fourier method, *J. Comput. Acoust.*, 21, 1250018, [dx.doi.org/10.1142/S0218396X1250018X](http://dx.doi.org/10.1142/S0218396X1250018X), 2013. [published, refereed]
- Lin, Y.-T., T. F. Duda, C. Emerson, G. Gawarkiewicz, A. E. Newhall, B. Calder, J. F. Lynch, P. Abbot, Y.-J. Yang and S. Jan, Experimental and numerical studies of sound propagation over a submarine canyon northeast of Taiwan, *IEEE J. Oceanic Eng.*, in press, 2014, <http://dx.doi.org/10.1109/JOE.2013.2294291>. [in press, refereed]
- Lin, Y.-T., K. G. McMahon, J. F. Lynch, and W. L. Siegmann, Horizontal ducting of sound by curved nonlinear internal gravity waves in the continental shelf areas, *J. Acoust. Soc. Am.*, 133, 37-49, [dx.doi.org/10.1121/1.4770240](http://dx.doi.org/10.1121/1.4770240), 2013. [published, refereed]
- Lynch, J. F., T. F. Duda and J. A. Colosi, Acoustical horizontal array coherence lengths and the “Carey Number”, *Acoustics Today*, 10, 10-19, <http://dx.doi.org/10.1121/1.4870172>, 2014. [published, not refereed]
- Lynch, J. F., T. F. Duda, W. L. Siegmann, J. Holmes and A. E. Newhall, The Carey Number in shallow water acoustics, in *Proceedings of the 1st International Underwater Acoustics Conference, Corfu, Greece, 2013*. [published, not refereed]
- Lynch, J. F., Y.-T. Lin, T. F. Duda and A. E. Newhall, Characteristics of acoustic propagation and scattering in marine canyons, in *Proceedings of the 1st International Underwater Acoustics Conference, Corfu, Greece, 2013*. [published, not refereed]
- Nash, J., S. Kelly, E. Shroyer, J. Moum and T. Duda, The unpredictability of internal tides in coastal seas, In *Proc. 7th International Symposium on Stratified Flows, Rome, Italy, 2011*. [published, not refereed]
- Nash, J. D., S. M. Kelly, E. L. Shroyer, J. N. Moum, and T. F. Duda, The unpredictable nature of internal tides and nonlinear waves on the continental shelf, *J. Phys. Oceanogr.*, 42, 1981-2000, [dx.doi.org/10.1175/JPO-D-12-028.1](http://dx.doi.org/10.1175/JPO-D-12-028.1), 2012. [published, refereed]
- Nash, J. D., E. L. Shroyer, S. M. Kelly, M. E. Inall, T. F. Duda, M. D. Levine, N. L. Jones, and R. C. Musgrave, Are any coastal internal tides predictable? *Oceanography*, 25, 80-95, <http://dx.doi.org/10.5670/oceanog.2012.44>, 2012. [published, refereed]

- Pan, Y. and D. Yue, Direct numerical investigation of turbulence of capillary waves, *Phys. Rev. Lett.*, 113, 094501, 2014. [published, refereed]
- Pan, Y. & Yue, D. 2015 Decaying capillary wave turbulence under broad-scale dissipation. *J. Fluid Mech.*, 780. [published, refereed]
- Paoletti, M. S., and H. L. Swinney, Propagating and evanescent internal waves in a deep ocean model, *J. Fluid Mech.*, 108, 148101, [dx.doi.org/10.1017/jfm.2012.284](http://dx.doi.org/10.1017/jfm.2012.284), 2012. [published, refereed]
- Paoletti, M. S., M. Drake, and H. L. Swinney, Internal tide generation in nonuniformly stratified deep oceans, *J. Geophys. Res. Oceans*, 119, 1953-1956, <http://dx.doi.org/10.1002/2013JC009469>, 2014. [published, refereed]
- Phadnis, A., Uncertainty Quantification and Prediction for Non-autonomous Linear and Nonlinear Systems. SM Thesis, Massachusetts Institute of Technology, Department of Mechanical Engineering, July 2013. [published, not refereed]
- Raghukumar, K., and J. A. Colosi, High frequency normal mode statistics in a shallow water waveguide: The effect of random linear internal waves, *J. Acoust. Soc. Am.* 136 , 66-79, <http://dx.doi.org/10.1121/1.4881926>, 2014. [published, refereed]
- Raghukumar, K., and J. A. Colosi, The effect of surface and linear internal waves on higher order acoustic moments in shallow water, *Proc. Meet. Acoust.*, 19, 070022, 2013. [published, not refereed]
- Raghukumar, K., and J. A. Colosi, High frequency normal mode statistics in shallow water: The combined effect of random surface and internal waves, *J. Acoust. Soc. Am.* 137, 2950-2961, <http://dx.doi.org/10.1121/1.4919358>, 2014. [published, refereed]
- Subramani, D. N. and P. F. J. Lermusiaux, 2015. Energy-based path planning by stochastic dynamically orthogonal level-set optimization. *Ocean Modeling*, in review, 2015. [submitted]
- Tran, D. D., M. Andrews, and P. Ratilal, Probability distribution for energy of saturated broadband ocean acoustic transmission: Results from Gulf of Maine 2006 Experiment, *J. Acoust. Soc. Am.*, 132, 3659-3672, 2012. [published, refereed]
- Ueckermann, M. P. and P. F. J. Lermusiaux, Hybridizable discontinuous Galerkin projection methods for Navier-Stokes and Boussinesq equations. *J. Comput. Phys.*, in review, 2015 [submitted]
- Xiao, W., Y. Liu, G. Wu and D. K. P. Yue, Rogue wave occurrence and dynamics by direct simulations of nonlinear wave-field evolution, *J. Fluid Mech.*, 720, 357-392, 2013. [published, refereed]
- Zhang, L. and H. L. Swinney, Virtual seafloor reduces internal wave generation by tidal flow, *Phys. Rev. Lett.*, 112, 104502 doi: 10.1103/PhysRevLett.112.104502, 2014. [published, refereed]
- Zhang, W. G. and T. F. Duda, Intrinsic nonlinearity and spectral structure of internal tides at an idealized Mid-Atlantic Bight shelfbreak, *J. Phys. Oceanogr.*, 43, 2641-2660, 2013. [published, refereed]
- Zhang, W. G., T. F. Duda, and I. A. Udovydchenkov, Modeling and analysis of internal-tide generation and beam-like onshore propagation in the vicinity of shelfbreak canyons, *J. Phys. Oceanogr.*, 44, 834-849, 2014. [published, refereed]

## **HONORS/AWARDS/PRIZES**

Recipient: Timothy F. Duda, Woods Hole Oceanographic Institution

Award Name: Editors' Citation for Excellence in Refereeing - Journal of Geophysical Research  
Oceans (2014)

Award Sponsor: American Geophysical Union

Recipient: Ying-Tsong Lin, Woods Hole Oceanographic Institution

Award Name A. B. Wood Medal and Prize of the Institute of Acoustics

Award Sponsor: Institute of Acoustics